Nanoscale

Accepted Manuscript

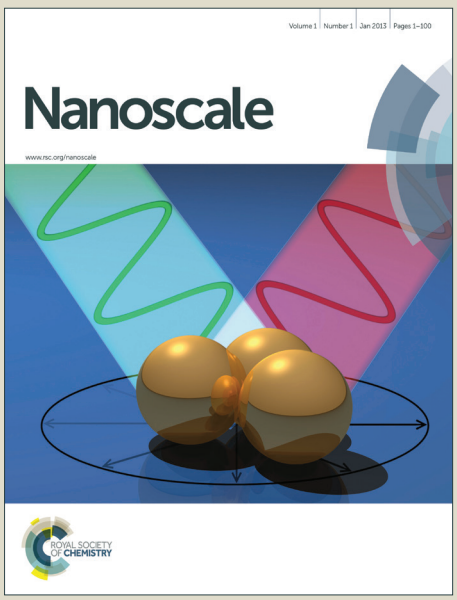

ROYAL SOCIETY OF CHEMISTRY

www.rsc.org/nanoscale

Nanoscale

COMMUNICATION

Co-assembly of Cyclic Peptide Nanotube and Block Copolymer in Thin Films: Control the Kinetic Pathway

Received 00th January 20xx,
Accepted 00th January 20xx

DOI: 10.1039/x0xx00000x

www.rsc.org/

Chen Zhang [a] and Ting Xu [a,b,c]

Directed co-assembly of polymer-conjugated cyclic peptide nanotube (CPN) and block copolymer in thin films is a viable approach to fabricate sub-nanometer porous membranes without synthesizing nanotubes with identical length and vertical alignment. Here we show that the process is pathway dependent and successful co-assembly requires eliminating CPN larger than 100 nm in solution. Optimizing polymer-solvent interaction can improve conjugate dispersion to certain extent, but this limits thin film fabrication. Introduction of a trace amount of hydrogen-bond blockers, such as trifluoroacetic acid by vapor absorption is more effective to reduce CPN aggregation in solution and circumvents issues with solvent immicibility. This study provides critical insights for guided assemblies within nanoscopic frameworks toward sub-nanometer porous membranes.

Membranes with uniform pore size less than 1 nm are desirable for molecular separation.[1, 2] Organic nanotubes such as cyclic peptides nanotubes (CPNs) are advantageous because the channel diameter and interior functionality can be molecularly tailored.[3-11] The guided growth of CPNs within cylindrical block copolymer (BCP) in thin films opened a viable approach to generate porous membrane with vertically aligned, uniform sub-nanometer channel with interior functionalization.[12] It overcame challenges of reducing pore size in nanoporous BCP membranes,[13-17] and synthesizing high aspect ratio nanotubes with controlled length and vertical alignment.[18, 19] In the guided CPN growth process, it was proposed that cyclic peptides (CPs) or short CPN tubelets need to be first selectively incorporated into BCP cylinders, and subsequently reassembled into high aspect ratio CPNs.[12] However, CPs and CPN tubelets tend to aggregate due to multi-pair inter-CP hydrogen bonding.[3, 20] When the aggregate size exceeds the periodicity of the BCP, the conjugate cannot be distributed uniformly within the preferred BCP microdomain, similar to what have been observed in nanoparticles/BCP blends.[21-23] The presence of large aggregates also compromises membrane quality and integrity, analogous to defects due to inorganic particles in composite membranes.[24, 25] Therefore, it is a requisite to develop systematic understanding in the kinetic pathway of the co-assembly process and to control CPN aggregation.

Polymers attached to the CPN exterior greatly affect CPN formation and its solubility in different media.[11, 12, 20, 26-30] However, previous studies are based on CP-polymer conjugate mixtures with different number of polymer chains attached.[12] The CP-polymer conjugates are purified via dialysis and there could be some trace amounts of chemical impurities. Here we developed purification procedure using Reversed-Phase High-Pressure Liquid Chromatography (RP-HPLC) to obtain model CP-polymer conjugates with high purity. The conjugate used is called "AK_4-4P2K", where four poly(ethylene glycol) (PEG) chains are attached to the lysine residues of CP with sequence AKAKAKAK (AK_4). To ensure the conjugate used contains well-defined architecture, PEG with molecular weight 2,000 Da was selected as other molecular weights resulted in either incomplete conjugation reaction or difficulty in purification. The conjugate purity was confirmed using mass spectrometry and analytical HPLC (Fig. 1). The RP-HPLC spectrum of the reaction mixture is shown in Fig. S1, *Supporting Information*. Only a single peak can be observed in Fig. 1b), confirming the purity of the conjugate. Cylindrical BCP, polystyrene (57 kDa)-block-poly(methyl methacrylate) (25 kDa) (PS-*b*-PMMA) was used as the nanoscopic framework to guide CPN growth. Thin films ~40 nm thick were prepared from toluene solution with

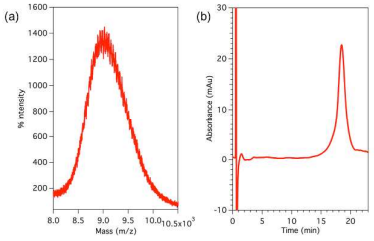

Figure 1. Characterization of purified AK_4-4P2K conjugate from reaction mixture. a) MALDI-TOF spectrum and b) corresponding RP-HPLC trace of the isolated AK_4-4P2k, confirming the purity of materials used in this study.

[a] *Department of Materials Science and Engineering, University of California, Berkeley, CA 94720-1760*
[b] *Department of Chemistry, University of California, Berkeley, CA 94720-1460*
[c] *Material Science Division, Lawrence Berkeley National Laboratory, Berkeley, CA 94720*

Electronic Supplementary Information (ESI) available: [details of any supplementary information available should be included here]. See DOI: 10.1039/x0xx00000x

constant BCP concentration at 10 mg/mL and varying conjugate concentration to tailor the fraction of AK_4-4P2K, *f*.

As shown previously, there is a reasonable agreement between the Atomic Force Microscopy (AFM) image and High-angle Annular Dark Field-Scanning Transmission Electron Microscopy (HAADF-STEM) results in terms of CPN formation in thin films.[12] Considering the limited area scanned and the time required to obtain high quality HAADF-STEM, present studies rely on AFM, in-plane TEM, and Grazing Incident Small-angle X-ray Scattering (GISAXS) for structural characterization.

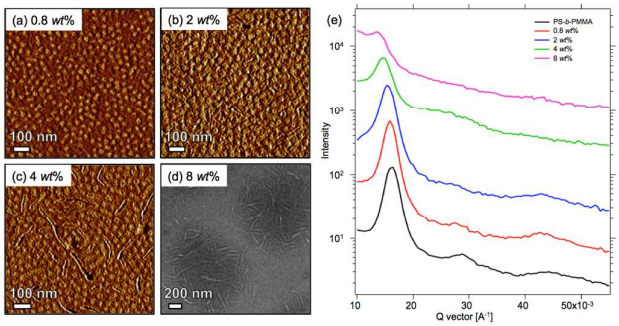

Figure 2. AFM phase images of blends of AK_4-4P2K conjugate and PS-*b*-PMMA in thin films with *f* at (a) 0.8 *wt%*, (b) 2 *wt%*, (c) 4 *wt%*, and (d) TEM image at 8 *wt%*. (e) shows the GISAXS profiles of the films. A left-shift in the first order peak position indicates the incorporation of AK_4-4P2K conjugate. The BCP lateral ordering deteriorates for thin films containing 8 *wt%* AK_4-4P2K.

Fig. 2 shows the AFM and TEM images of thin films containing different fraction of AK_4-4P2K after thermal annealing at 180°C for 4hr in vacuum. At 0.8 *wt%*, homogeneous morphology is observed where cylindrical PMMA microdomains are oriented normal to the substrate. Dark circular areas ~3-5 nm, which are confirmed previously to be the PEG-covered CPNs can be seen at the center of some PMMA cylinders,[12] indicating that only a fraction of PMMA microdomains contains CPNs. At 2 or 4 *wt%*, CPNs are seen in most vertically aligned PMMA cylinders. However, there are aggregates of PEG-covered CPNs on the surface for both films. At *f* = 8 *wt%*, the top-view TEM image shows the film contains a large fraction of PEG-covered CPNs laying parallel to the surface. GISAXS was used to characterize the in-plane ordering and to quantify the average lateral periodicity (L_o). As *f* increases, the first order peak shifts to a lower Q (scattering vector) value, and L_o increases from 38.4 nm for BCP alone, to 39.5 nm and 40.6 nm for 0.8 and 2 *wt%*, respectively. This, in conjunction with the AFM results and previous HAADF-STEM studies, indicates the incorporation of PEG-covered CPNs in the PMMA cylinders. The diffraction peak also broadens as *f* increases, implying less in-plane ordering. The ordered cylinder morphology is largely lost when *f* >4 *wt%*, consistent with the TEM result.

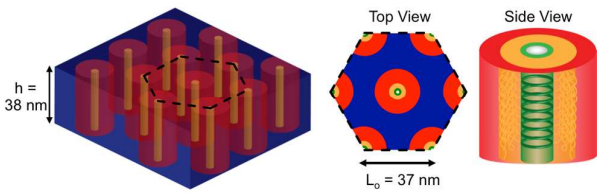

Figure 3. Schematic illustrating the estimation of AK_4-4P2k loading limit in cylindrical BCP. Under the constraint of the hydrogen bond distance and known film thickness, each PMMA cylinder contains ~ 8 cyclic peptides stacked vertically, resulting in an estimated loading limit ~ 2.6 wt%.

A simple model shown in Fig. 3 is used to investigate the loading limit of the system and details are outlined in Fig. S4 , *SI*. More than one CPN in one PMMA microdomain is not considered here due to high energy cost to deform PMMA cylinders and rearrangement of cylindrical BCPs.[31] The critical *f* value for one PEG-covered CPN per PMMA cylinder is ~2.6 *wt%*. However, aggregates (darker regions) are still seen at 2 *wt%* film (Fig. 2b). Thus, the aggregation cannot be explained by the CPN loading limit within PMMA cylinder alone.

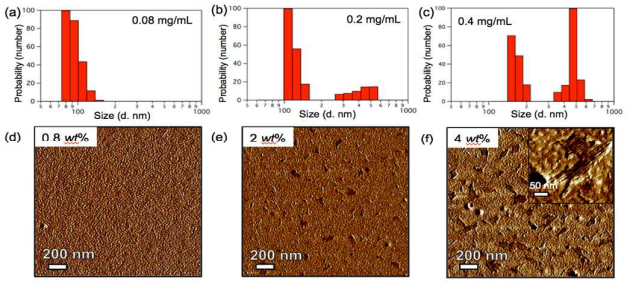

Figure 4. DLS results of AK_4-4P2K conjugates in toluene at various concentrations (a) 0.08 mg/mL, (b) 0.2 mg/mL, (c) 0.4 mg/mL; and corresponding AFM phase images of as-casted AK_4-4P2K conjugates in BCP at the same *f* values, respectively. Increasing solution concentration of AK_4-4P2K conjugates results in larger aggregates in toluene. The inset of (f) shows the details of the AK_4-4P2K aggregates consisted of bundles of PEG-covered CPNs.

Dynamic light scattering (DLS) studies (Fig. 4) confirm that the AK_4-4P2K conjugates pre-aggregate in toluene prior to thin film formation. Homogeneous morphology is only seen for conjugates < 100 nm at 0.8 *wt%* (Fig. 2a). The sizes increase from ~ 100-400 nm at 2 *wt%* to ~200-600 nm at 4 *wt%*. After further annealing at 245°C (Fig. 5) while the thin film still remains intact, the CPN aggregates are only partially broken. Less CPN aggregates are seen on the surface comparing to the sample annealed at 180°C (Fig. 2b), but surface defects of lay-down PEG covered CPNs still remain. Although the study clearly demonstrates the exceptional thermal stability of polymer-covered CPNs,[11, 12] the surface defects due to CPN aggregation are undesirable and need to be eliminated.

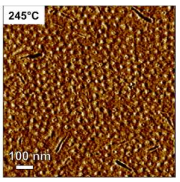

Figure 5. AFM image of 2 *wt%* sample annealed at 245°C below BCP degradation temperature.

The CPN aggregation can be attributed to two factors: strong hydrogen bonding between CP rings,[3] and interactions between the attached polymers and the solvent.[20] Molecular dynamic simulation studies show there are 7-8 pairs of hydrogen bonds between CPs,[11, 32, 33] which are the main force stabilizing CPN and contributors to the insolubility of CPNs in most organic solvents. Polymers covalently attached to the CPN exterior can improve solubility and modulate CPN growth.[20, 26-28] While toluene, with solubility parameter δ=8.9 $(calcm^{-3})^{-1/2}$, is good for preparing smooth thin films of PS-*b*-PMMA, it is not a good solvent for PEG (δ=9.9), leading to aggregation of PEG-covered CPNs in solution.[34] DLS studies (Fig. 6a,b) show that benzene (δ=9.1) and chloroform (δ=9.2)

are more effective in solubilizing AK_4-4P2K and reducing the aggregate size down to ~70 nm and ~200-300 nm, respectively. In contrast, poor solvent such as o-xylene (δ=8.85) results in aggregates of a few micrometers (Fig. 6c). For benzene in particular, homogeneous as-cast film is obtained at 2 *wt%* when the conjugate size is < 100nm, and well-aligned CPNs at the center of PMMA cylinder can be seen post thermal annealing (Fig. 6d).

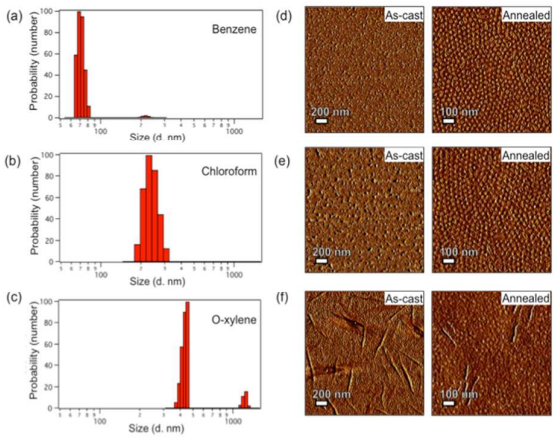

Figure 6. DLS results of 0.4 mg/mL AK_4-4P2K conjugate solutions in (a) benzene, (b) chloroform, (c) o-xylene; and AFM phase images of as-casted and annealed AK_4-4P2k /BCP blends at f = 2 *wt%* casted from (d) benzene, (e) chloroform, and (f) o-xylene, respectively. Favorable PEG-solvent interactions result in better dispersion of AK_4-4P2K conjugates in solution.

Although tailoring solvent-polymer interaction is effective, it limits solvent selection and benzene is not ideal due to its toxicity. An alternative approach was developed to reduce inter-CP hydrogen bonds during thin film fabrication. Trifluoroacetic acid (TFA) is one of the very few polar solvents used to dissolve CPs.[3, 20, 26] In prior solution studies, TFA was mixed with polar solvents such as DMF to disperse CP or CP-polymer conjugates in solution.[20, 35] However, none of these polar solvents are suitable for polymer processing, and TFA is incompatible with many organic solvents. To overcome the miscibility issue, we developed a simple yet effective route to introduce TFA as co-solvent. The freshly lyophilized AK_4-4P2K powder was first exposed to TFA vapor (Fig. S6, *SI*) and then co-dissolved in toluene with PS-*b*-PMMA, and the solution remained clear. Fourier Transform Infrared spectra (FTIR) of samples pre-/post treatment are shown in Fig. 7a. The characteristic peak ~1200 cm^{-1} corresponding to C-F bond can be clearly seen for AK_4-4P2K and PEG post TFA exposure. To quantitatively estimate the amount of TFA absorbed, 19F Nuclear Magnetic Resonance spectroscopy (NMR) was used. Shown in Fig. S3a of the *SI*, using 2,2,2-trifluoroethanol (TFE) as reference, 1 mg of AK_4-4P2k absorbs ~ 0.394 mg of TFA. Based on FTIR spectra, we speculate that PEG chains molecularly absorb TFA, and act as a local TFA reservoir. The amount of TFA present is sufficient to prevent CPN aggregation in toluene. The DLS result in Fig. 4b shows the size of CPN aggregate is ~200 nm in TFA treated toluene, while large aggregates ~400 nm are seen in untreated solution. Thermal annealing removes most TFA molecules to the level below the detection limit as indicated by the disappearance of the C-F peak after heating (Fig. 7a, solid blue trace), and the lack of TFA peak in NMR spectrum (Fig. S3b, *SI*). More importantly, no CPN aggregates are seen in the as-cast film (Fig. 7c), and well-aligned CPN channels are formed in PMMA cylinders post thermal annealing (Fig. 7d).

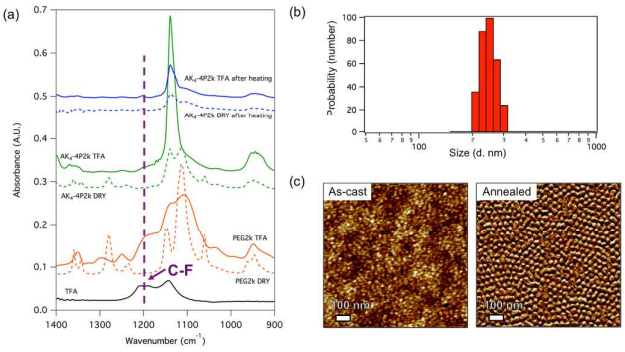

Figure 7. (a) FTIR spectra of various samples at room temperature, (b) DLS result of 0.4 mg/mL AK_4-4P2k post TFA treatment in toluene, and (c) AFM images of (b) blended with BCP at f=2 *wt%*. TFA molecules, removable by thermal heating, are absorbed to the conjugates, reducing aggregation in toluene and resulting in well-aligned CPNs after annealing.

Conclusions

Guided growth of organic nanotube in polymeric matrix opens a viable route to fabricate sub-nanometer membranes by eliminating the need to control the nanotube diameter, length, and vertical alignment. However, CPNs tend to aggregate, preventing formation of through channels and compromising the membrane quality. Using well-defined CP-PEG conjugate with high purity, we systematically investigated the kinetic pathway of co-assembling the conjugate and cylindrical BCP in thin films and highlight important parameters to obtain high quality membrane. Thermal annealing at 245°C is ineffective in dispersing aggregates > 300 nm. Two routes were developed to overcome the membrane processing challenges. Using favorable solvents of PEG can reduce conjugate aggregation, thus improving the uniformity of vertically aligned CPN. The more effective route is to introduce a trace amount of small molecule hydrogen bond blocker, such as TFA to interfere with the inter-CP hydrogen bonding. Good nanotube dispersion is achieved even using non-optimal solvents for the polymer-covered nanotubes. The introduction of removable small molecule opens up a simple and yet viable route to modulate organic nanotube assembly during the fabrication process.

Experimental

Materials

The linear sequence of octapeptide [D-Ala-L-Lys]$_4$ (AK_4) was synthesized following standard 9-fluorenylmethoxycarbonyl (Fmoc) protocols for solid-phase peptide synthesis using 2-chlorotrityl chloride resin preloaded with Fmoc-D-Ala-OH. The linear peptide was then cleaved from the resin and cyclized head-to-tail using propylphosphonic anhydride (T3P, Sigma

Aldrich) and N,N-Diisopropylethylamine (DIPEA, Sigma Aldrich) in DMF. Boc-protecting groups on lysine residues were removed by 95% TFA to expose the free amines. Carboxylic acid-terminated PEG was conjugated to AK_4 at a ratio of 4 PEG : 1 CP. 1-ethyl-3-(3-dimethylaminopropyl) carbodiimide (EDC) was used as the coupling reagent and the reaction was run in MES buffer at pH 6.5. Fmoc-D-Ala-OH, Fmoc-L-Lys(Boc)-OH, polystyrene-(2-chlorotrityl) resin (loading: 1.5 mmol/g), and 2 - (6-Chloro-1H-benzotriazole-1-yl)- 1,1,3,3 - tetramethylaminium hexafluorophosphate (HCTU) were purchased from Nova Biochem. Polystyrene-*b*-poly(methyl methacrylate) (57K-25K, PDI 1.07) was purchased from Polymer Source. Carboxylic acid-terminated PEG (Mw=2K, PDI 1.2) was purchased from RAPP POLYMERE. All reagents were purchased with the highest purity and used as received unless otherwise noted. The random copolymers of styrene and methyl methacrylate with 2% reactive benzocyclobutene (BCB) [P(S-*r*-BCB-*r*-MMA)] (Mw= 45K PDI 1.3) was provided by T. P. Russell at the University of Massachusetts, Amherst.

Grazing Incident Small Angle X-ray Scattering (GISAXS)
Measurements were performed at beamline 8-ID Advanced Photon Source (APS) at Argonne National Lab with x-ray wavelength 1.240 nm.

Dynamic Light Scattering (DLS)
DLS was performed using Brookhaven BI-200SM at a wavelength of 637 nm with the scattering angle at 90°. The solvent used was filtered using 0.1 µm PTFE filters.

Fourier Transfer Infrared Spectroscopy (FTIR)
FTIR measurements were performed using Perkin Elmer Spotlight 200 FTIR Microscope System. Samples were prepared by casting toluene solutions between two NaCl pellets.

Acknowledgements

This work was supported by the National Science Foundation through grant CBET-1235439. Initial exploration of TFA study was supported by ARO W91NF-09-1-0374. GISAXS measurements were carried out at beamline 7.3.3 at the Advanced Light Source at Lawrence Berkeley National Laboratory, and 8-ID at Advanced Photon Source at Argonne National Laboratory. We thank T. Yee for assisting the synthesis of AK_4-4P2K and Dr. Y. Qiu for valuable discussions.

Notes and references

1. D. L. Gin and R. D. Noble, *Science*, 2011, **332**, 674-676.
2. M. A. Shannon, P. W. Bohn, M. Elimelech, J. G. Georgiadis, B. J. Marinas and A. M. Mayes, *Nature*, 2008, **452**, 301-310.
3. M. R. Ghadiri, J. R. Granja, R. A. Milligan, D. E. Mcree and N. Khazanovich, *Nature*, 1993, **366**, 324-327.
4. M. R. Ghadiri, J. R. Granja and L. K. Buehler, *Nature*, 1994, **369**, 301-304.
5. J. R. Granja and M. R. Ghadiri, *J Am Chem Soc*, 1994, **116**, 10785-10786.
6. N. Khazanovich, J. R. Granja, D. E. McRee, R. A. Milligan and M. R. Ghadiri, *J Am Chem Soc*, 1994, **116**, 6011-6012.
7. J. D. Hartgerink, J. R. Granja, R. A. Milligan and M. R. Ghadiri, *J Am Chem Soc*, 1996, **118**, 43-50.
8. T. D. Clark, J. M. Buriak, K. Kobayashi, M. P. Isler, D. E. McRee and M. R. Ghadiri, *J Am Chem Soc*, 1998, **120**, 8949-8962.
9. M. Amorin, L. Castedo and J. R. Granja, *J Am Chem Soc*, 2003, **125**, 2844-2845.
10. W. S. Horne, C. D. Stout and M. R. Ghadiri, *J Am Chem Soc*, 2003, **125**, 9372-9376.
11. R. Hourani, C. Zhang, R. van der Weegen, L. Ruiz, C. Y. Li, S. Keten, B. A. Helms and T. Xu, *J Am Chem Soc*, 2011, **133**, 15296-15299.
12. T. Xu, N. N. Zhao, F. Ren, R. Hourani, M. T. Lee, J. Y. Shu, S. Mao and B. A. Helms, *Acs Nano*, 2011, **5**, 1376-1384.
13. J. Rzayev and M. A. Hillmyer, *Macromolecules*, 2005, **38**, 3-5.
14. S. Y. Yang, I. Ryu, H. Y. Kim, J. K. Kim, S. K. Jang and T. P. Russell, *Adv Mater*, 2006, **18**, 709-712.
15. K.-V. Peinemann, V. Abetz and P. F. W. Simon, *Nat Mater*, 2007, **6**, 992-996.
16. E. A. Jackson and M. A. Hillmyer, *Acs Nano*, 2010, **4**, 3548-3553.
17. Y. Wang and F. Li, *Adv Mater*, 2011, **23**, 2134-2148.
18. J. K. Holt, H. G. Park, Y. Wang, M. Stadermann, A. B. Artyukhin, C. P. Grigoropoulos, A. Noy and O. Bakajin, *Science*, 2006, **312**, 1034-1037.
19. B. J. Hinds, N. Chopra, T. Rantell, R. Andrews, V. Gavalas and L. G. Bachas, *Science*, 2004, **303**, 62-65.
20. R. Chapman, M. L. Koh, G. G. Warr, K. A. Jolliffe and S. Perrier, *Chem Sci*, 2013, **4**, 2581-2589.
21. R. B. Thompson, V. V. Ginzburg, M. W. Matsen and A. C. Balazs, *Science*, 2001, **292**, 2469-2472.
22. A. C. Balazs, T. Emrick and T. P. Russell, *Science*, 2006, **314**, 1107-1110.
23. M. R. Bockstaller, R. A. Mickiewicz and E. L. Thomas, *Adv Mater*, 2005, **17**, 1331-1349.
24. M.-D. Jia, K.-V. Pleinemann and R.-D. Behling, *Journal of Membrane Science*, 1992, **73**, 119-128.
25. T.-S. Chung, L. Y. Jiang, Y. Li and S. Kulprathipanja, *Progress in Polymer Science*, 2007, **32**, 483-507.
26. J. Couet, J. D. Jeyaprakash, S. Samuel, A. Kopyshev, S. Santer and M. Biesalski, *Angew Chem Int Edit*, 2005, **44**, 3297-3301.
27. J. Couet and M. Biesalski, *Small*, 2008, **4**, 1008-1016.
28. M. G. J. ten Cate, N. Severin and H. G. Borner, *Macromolecules*, 2006, **39**, 7831-7838.
29. R. Chapman, K. A. Jolliffe and S. Perrier, *Adv Mater*, 2013, **25**, 1170-1172.
30. M. Danial, C. My-Nhi Tran, P. G. Young, S. Perrier and K. A. Jolliffe, *Nat Commun*, 2013, **4**.
31. U. Jeong, D. Y. Ryu, D. H. Kho, D. H. Lee, J. K. Kim and T. P. Russell, *Macromolecules*, 2003, **36**, 3626-3634.
32. E. Khurana, S. O. Nielsen, B. Ensing and M. L. Klein, *The Journal of Physical Chemistry B*, 2006, **110**, 18965-18972.
33. M. Engels, D. Bashford and M. R. Ghadiri, *J Am Chem Soc*, 1995, **117**, 9151-9158.
34. J. Brandrup and E. H. Immergut, *Polymer handbook*, Interscience Publishers, 1966.
35. R. Chapman, K. A. Jolliffe and S. Perrier, *Aust J Chem*, 2010, **63**, 1169-1172.